

The NLO QCD corrections to $B_c(B_c^*)$ production around Z pole at an e^+e^- collider

Xu-Chang Zheng^{a,c*}, Chao-Hsi Chang^{a,b,c†}, Tai-Fu Feng^{a,d‡}, Zan Pan^{a,c§}

^a Key Laboratory of Theoretical Physics, Institute of Theoretical Physics,
Chinese Academy of Sciences, Beijing 100190, China

^b CCAST (World Laboratory), P.O.Box 8730, Beijing 100190 China

^c School of Physical Sciences, University of Chinese Academy of Sciences, Beijing 100049, China and

^d Department of Physics, Hebei University, Baoding, 071002, China

Production of the B_c and B_c^* mesons at Z -factory (an e^+e^- collider running at energies around Z pole) is calculated up-to the next-to-leading order (NLO) QCD corrections. The results show that the dependence of the total cross sections on the renormalization scale μ is reduced by the corrections, and the NLO corrections enhance the production cross section by 52%(33%) when the renormalization scale is taken at $\mu = 2m_b$. For experimental observations of the B_c and B_c^* mesons, the differential cross sections for the production are also analyzed up-to the NLO accuracy.

Keywords: NLO QCD correction, B_c meson, production, e^+e^- collision

PACS numbers: 13.66.Bc, 12.38.Bx, 14.40.Pq, 14.70.Hp

I. INTRODUCTION

The meson B_c (and its anti-particle \bar{B}_c), as unique explicitly doubly heavy-flavored meson at ground state in the Standard Model (SM), has attracted a lot of interests since it was first observed by CDF collaboration[1]. Due to its doubly heavy flavored nature, the two heavy components inside it move non-relativistically and it can be described reliably by potential model[2], while its production may be described in terms of the effective theory of nonrelativistic quantum chromodynamics (NRQCD)[3] and its decays may be described by effective theory of weak interaction which is based on SM.

Since the fact that the discovery and the available observations are at high energy colliders, so the theoretical and experimental studies on B_c meson so far mainly have been concentrated on hadronic colliders with high luminosity[4, 5]. However, at a hadronic collider, the production of B_c meson is through collisions of partons inside the colliding hadrons, the longitudinal component of the momentum of the products and the center-of-mass system of the reaction as well cannot be determined, so only the perpendicular components of the momentum of the products can be measured and can be used for tests. Moreover, in hadronic colliders, there are always many hadrons in final state which relate to the initial hadrons but not relate to the subprocess of B_c meson production at all, and cause backgrounds only. On the contrary, there are less backgrounds at an e^+e^- collider, and the center-of-mass system of initial e^+e^- is well-controlled, so the momentum components of products as well as angle distribution of the concerned product can be used

to test theoretical prediction, thus to study B_c meson production at an e^+e^- collider is interesting. Based on the theoretical estimate and LEP-I experimental observation, the B_c meson production is small even running at the resonance of Z -boson[6, 7]. However, now several plans about Z -factories (e^+e^- colliders running at energies around Z pole with much higher luminosity than that of LEP-I), e.g. ILC, CEPC and FCC-ee, are under considering, thus we think that it is the time now to re-study the production of B_c by e^+e^- collisions. As pointed out in Ref.[8], the production of B_c by e^+e^- collisions, even at the energy of Z -pole through the Z -boson resonance, contains much more information than that the production from Z decay, thus in Ref.[8] we re-considered the production thoroughly, and now we consider its QCD corrections up-to the next order, although in the literature the production through Z -decay up-to the next order QCD corrections is considered in Refs.[9, 10]. Indeed, the calculation on the production for the e^+e^- collisions up-to the next order QCD corrections is more complicated than that for the production via Z decay.

According to NRQCD, the production of B_c meson in an electron-positron collider can be factorized into two parts: one is the production of free $c\bar{b}$ quark pair inclusively in short distance which can be calculated by perturbative QCD (pQCD), and the other one is that to form the meson B_c from the produced $c\bar{b}$ quark pair. The later is of nonperturbative nature, but can be determined phenomenologically or potential model etc. Whereas here we take into account the QCD corrections up-to next order on the former part and the later part (the factors) is kept only at the leading order in relative velocity v between the two heavy quarks inside the meson B_c .

To study the production of such a doubly heavy system (B_c meson) can help to understand the perturbative and nonperturbative QCD deeper. Since B_c carries two heavy-flavors explicitly, its excited states will decay to B_c through strong or electromagnetic interaction with almost 100% probability, thus, here we also study the

*e-mail:zhengxc@itp.ac.cn

†e-mail:zhangzx@itp.ac.cn

‡email:fengt@hbu.edu.cn

§e-mail:panzan@itp.ac.cn

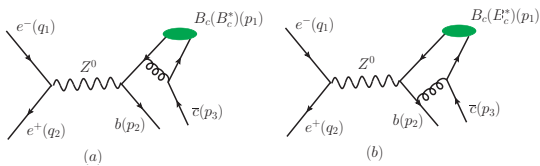


FIG. 1: Two of four LO Feynman diagrams for the process $e^-(q_1) + e^+(q_2) \rightarrow B_c(B_c^*)(p_1) + b(p_2) + \bar{c}(p_3)$.

production of B_c^* ($^3S_1, J^P = 1^-$, the lowest excited state of B_c) so as to understand some of the excited state production. The study of the production and decay of these excited states is also interesting.

As mentioned above, recently in Ref.[8] we have studied the production of doubly heavy flavored hadrons (B_c meson and baryons $\Xi_{cc}, \Xi_{bc}, \Xi_{bb}$ etc and their excited states as well as their antiparticle) at e^+e^- colliders. It is found that if one wishes to study B_c meson (and its excited states) thoroughly, then the e^+e^- collider should run at the Z pole with a very luminosity, such as $10^{35} \text{cm}^{-2}\text{s}^{-1}$ even higher. In Ref.[8] we studied the total cross section as well as the differential cross sections relating to outgoing angles and energy of the produced B_c meson (and its excited states) under complete QCD approach to leading order (LO) and fragmentation approach to leading logarithm order (LL). However, the LO results have remarkable dependence on the renormalization scale. These make the LO results bring in considerable uncertainty. In order to give a more precise theoretical prediction and to see the dependence on the renormalization scale, in this paper, we calculate the B_c (and B_c^*) meson production at an e^+e^- collider, which runs near the Z pole, up-to the NLO corrections of QCD under the complete QCD approach.

The paper is organised as follows: Following the Introduction, in Section II, we present the brief formulas on which the LO calculations are based. In Section III, we present the approaches to compute the NLO corrections of QCD for the B_c (and B_c^*) meson production at e^+e^- colliders. In Section IV, we present the numerical results. Section V is reserved for discussions and summary.

II. LO LEVEL CROSS SECTION

There are four Feynman diagrams for the $B_c(B_c^*)$ meson production at LO, two of them have been shown in

A. The NLO QCD virtual correction

The virtual correction up-to NLO of QCD is the contributions from the interference of the LO ones with the correction Feynman diagrams, i.e. Figs.2,3,4,5 and those of these diagrams with the c -quark and b -quark lines be-

ing interchanged. Thus the correction to the cross section can be formulated as

The cross section up-to LO QCD can be formulated as:

$$d\sigma_{\text{LO}} = \frac{1}{4} \frac{1}{2s} \sum |M_{\text{LO}}|^2 d\Phi_3, \quad (1)$$

where $\frac{1}{2s}$ is the flux factor. \sum means that the spins and the colors in the initial and final states are summed over. $1/4$ comes from the spin average of initial e^+e^- . $d\Phi_3$ denotes the three-body phase space for the final states. M_{LO} is the LO Feynman amplitude, which is the sum of four terms relating to the LO Feynman diagrams. The details about M_{LO} can be found in Ref.[8].

III. THE NLO QCD CORRECTIONS

The NLO QCD corrections to the process $e^+ + e^- \rightarrow B_c(B_c^*) + b + \bar{c}$ include virtual and real corrections. Half of the Feynman diagrams for virtual correction can be found in Figs.2,3,4,5, and half of the Feynman diagrams for real correction can be found in Fig.6. The other half of the Feynman diagrams for virtual and real corrections can be easily obtained by interchanging the b -quark and c -quark lines in Figs.2~6. To the NLO QCD accuracy, the cross section is formulated as

$$\sigma_{\text{NLO}} = \sigma_{\text{LO}} + \sigma_{\text{Virtual}} + \sigma_{\text{Real}}. \quad (2)$$

Here σ_{Virtual} denotes the so-called virtual correction and σ_{Real} denotes the so-called real correction. Now let us calculate them respectively.

ing interchanged. Thus the correction to the cross section can be formulated as

$$d\sigma_{\text{Virtual}} = \frac{1}{4} \frac{1}{2s} \sum 2\text{Re}(M_{\text{LO}}^* M_{\text{Virtual}}) d\Phi_3. \quad (3)$$

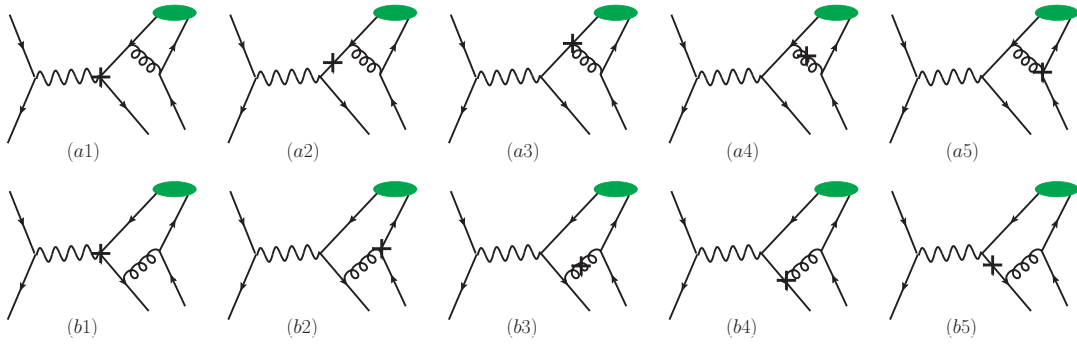


FIG. 2: Half of the counterterm diagrams for the process $e^- + e^+ \rightarrow B_c(B_c^*) + b + \bar{c}$.

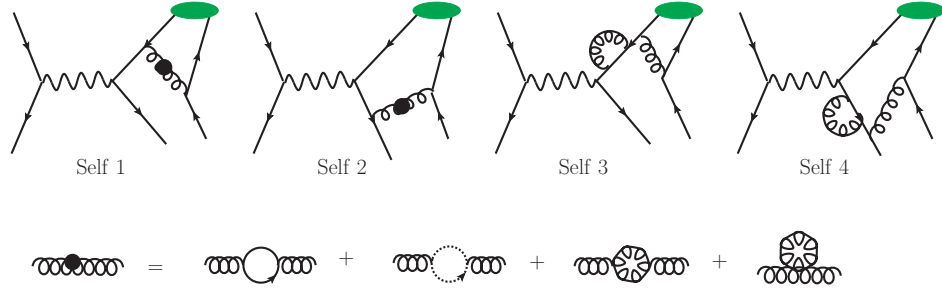


FIG. 3: Half of self-energy diagrams in virtual corrections.

There are ultraviolet (UV) and infrared (IR) divergences in the amplitudes relating to the correction diagrams. We adopt dimensional regularization with $D = 4 - 2\epsilon$ to isolate the UV and IR divergences. There are the Coulomb divergences in the conventional matching procedure, which should be absorbed into the binding potential for the two heavy quarks inside the meson B_c . In the dimensional regularization, there is a simpler way to extract the NRQCD short-distance coefficients directly using the method of regions[11], i.e., expanding the amplitudes with the relative momentum (q) of the constituent quarks before performing loop integration, and in the lowest non-relativistic approximation for the S -wave states of the binding system $c\bar{b}$, only the terms with $q = 0$ are taken. Thus we don't confront the contributions from the low energy regions such as those from the potential region.

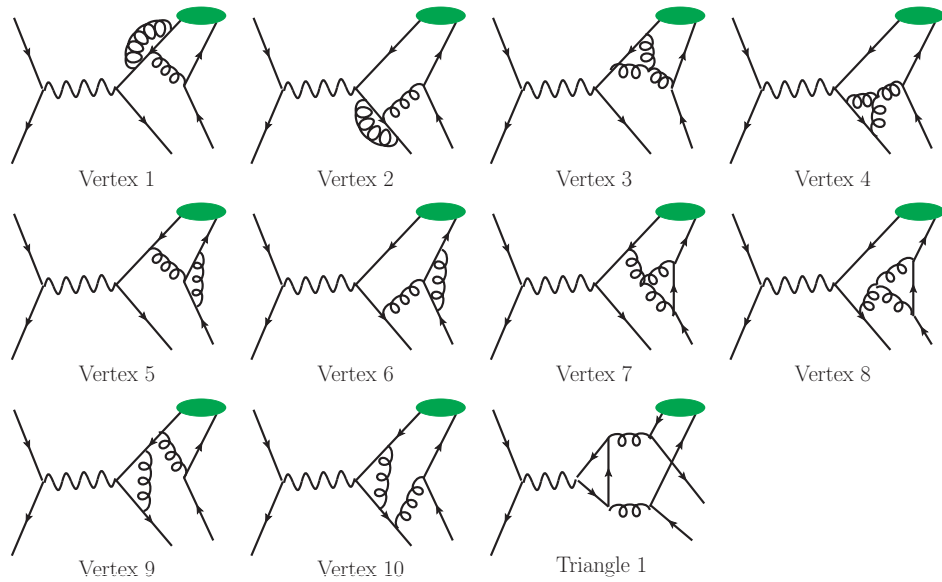


FIG. 4: Half of vertex and triangle diagrams in virtual corrections.

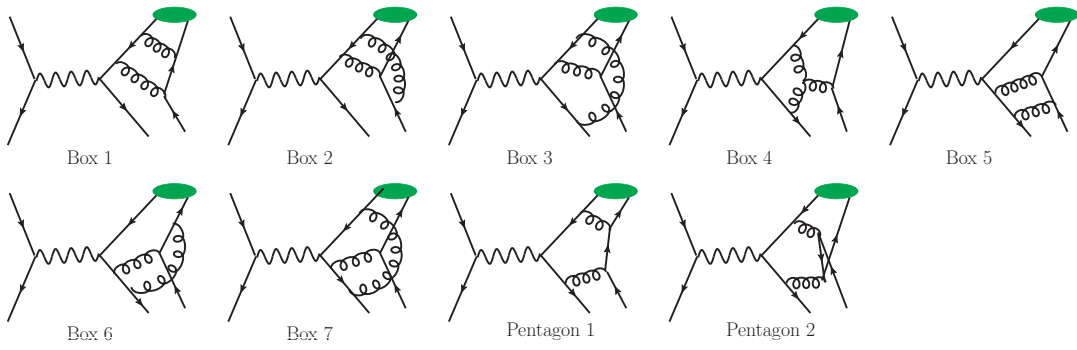


FIG. 5: Half of box and pentagon diagrams in virtual corrections.

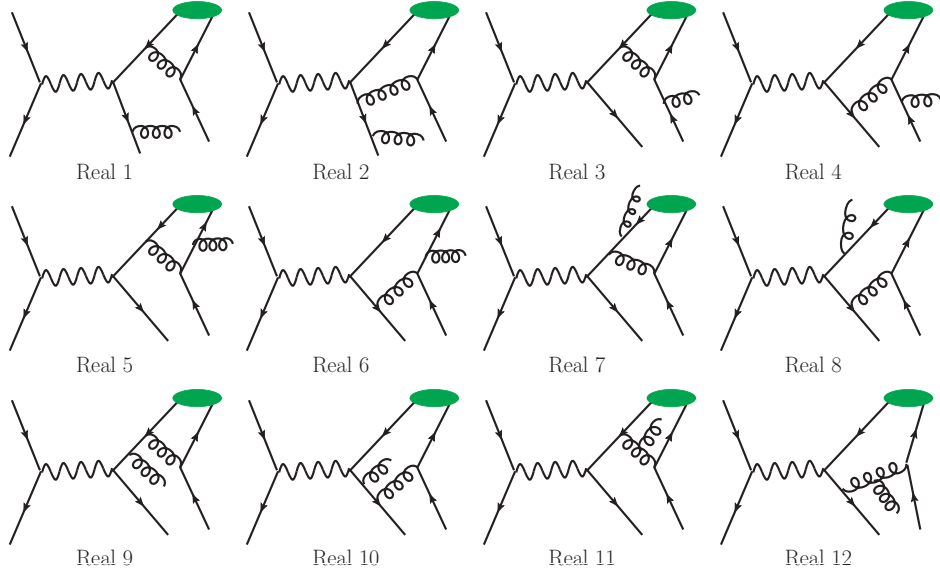


FIG. 6: Half of the Feynman diagrams in real corrections.

In dimensional regularization, γ_5 should be treated carefully. We adopt the reading point prescription[12]. It has the following rules,

- The anticommutation relation $\{\gamma_5, \gamma^\mu\} = 0$ is valid. Thus after applying the anticommutation relation and $\gamma_5^2 = 1$, there is one or no γ_5 in each Dirac trace.
- Cyclic manipulation in the Dirac traces is prevented. When considering the contributions from several diagrams, for all of them the traces in the amplitude (or resulting from squared fermionic amplitudes) must be read with starting from the same vertex respectively.
- The relevant axial current anomalies would be obtained and the conservation for vector currents is guaranteed by starting all the traces with the axial vector vertex.

Here the UV divergences come from self-energy, vertex and triangle diagrams only¹, which are canceled by the counter terms through renormalization, and here the renormalization scheme is that the renormalization constants Z_2 , Z_m , and Z_3 , which correspond to the renormalization of quark field, quark mass and gluon field, are determined by the renormalization of the on-mass-shell scheme (OS), whereas Z_g relating to the strong coupling constant α_s is determined by the renormalization of the modified-minimal-subtraction scheme (\overline{MS}). Then with

¹ The UV divergence from the amplitude of the anomalous diagram Triangle-1 in Fig.4 is canceled by the UV divergence from the other anomalous diagram.

the renormalization, we have:

$$\begin{aligned}
\delta Z_2^{OS} &= -C_F \frac{\alpha_s}{4\pi} \left[\frac{1}{\epsilon_{UV}} + \frac{2}{\epsilon_{IR}} - 3\gamma_E + 3 \ln \frac{4\pi\mu^2}{m^2} + 4 \right], \\
\delta Z_m^{OS} &= -3 C_F \frac{\alpha_s}{4\pi} \left[\frac{1}{\epsilon_{UV}} - \gamma_E + \ln \frac{4\pi\mu^2}{m^2} + \frac{4}{3} \right], \\
\delta Z_3^{OS} &= \frac{\alpha_s}{4\pi} \left[(\beta'_0 - 2C_A) \left(\frac{1}{\epsilon_{UV}} - \frac{1}{\epsilon_{IR}} \right) \right. \\
&\quad \left. - \frac{4}{3} T_F \left(\frac{1}{\epsilon_{UV}} - \gamma_E + \ln \frac{4\pi\mu^2}{m_c^2} \right) \right. \\
&\quad \left. - \frac{4}{3} T_F \left(\frac{1}{\epsilon_{UV}} - \gamma_E + \ln \frac{4\pi\mu^2}{m_b^2} \right) \right], \\
\delta Z_g^{\overline{MS}} &= -\frac{\beta_0}{2} \frac{\alpha_s}{4\pi} \left[\frac{1}{\epsilon_{UV}} - \gamma_E + \ln(4\pi) \right], \tag{4}
\end{aligned}$$

where m appearing in δZ_2^{OS} and δZ_m^{OS} represents the mass m_b or m_c accordingly, μ is the energy where the renormalization is to carry out, and γ_E is Euler's constant. $\beta_0 = \frac{11}{3}C_A - \frac{4}{3}T_F n_f$ is the one-loop coefficient of the QCD β -function, and n_f is the number of active quark flavors. Here for the concerned process, there are three light quarks u, d, s and two heavy quarks c, b , so $n_f = 5$. But in Eq.(4) precisely $\beta'_0 = \frac{11}{3}C_A - \frac{4}{3}T_F n_{lf}$, and $n_{lf} = 3$ for the light quark flavors. For $SU(3)_c$ group, $C_A = 3$, $T_F = \frac{1}{2}$ and $C_F = \frac{4}{3}$. Because there is no external gluon line at LO level, δZ_3 is canceled at NLO total amplitude level, so the final results are independent of the renormalization scheme of the gluon field.

According to Refs.[13, 14], the IR divergences in the Feynman diagrams for the virtual corrections can be well analyzed. For the concerned process, the IR divergences come from the vertex, box and pentagon diagrams. Of Fig.4, only the amplitudes corresponding to diagrams Vertex-5 and Vertex-6 have IR divergences. Of Fig.5, except Box-4, the rests have IR divergences². The other half of the Feynman diagrams, which are obtained from Figs.4~5 by interchanging the c -quark and b -quark lines, have similar IR divergences. The IR divergences in the virtual correction will be canceled by the IR divergences from counter terms and real corrections.

B. The real correction for NLO

Note that here 'the NLO real correction' for the concerned process $e^-(q_1) + e^+(q_2) \rightarrow B_c(B_c^*)(p_1) + b(p_2) + \bar{c}(p_3)$ means to take into account the full contributions from the process $e^+e^- \rightarrow B_c(B_c^*) + b + \bar{c} + g$ with the gluon in final state covering whole possible phase space³.

Half of the Feynman diagrams for the real correction are shown in Fig.6 and the other half can be obtained from Fig.6 through interchanging the c -quark and b -quark lines. The correction to the relevant cross section can be written as:

$$d\sigma_{\text{Real}} = \frac{1}{4} \frac{1}{2s} \sum |M_{\text{Real}}|^2 d\Phi_4, \tag{5}$$

where M_{Real} is the sum of 24 terms relating to the 24 Feynman diagrams for the real correction. $|M_{\text{Real}}|^2$ can be formulated as

$$|M_{\text{Real}}|^2 = \sum_{i,j} M_{\text{Real},i}^* M_{\text{Real},j}, \tag{6}$$

where i, j vary from 1 to 24 corresponding to the 24 real correction Feynman diagrams.

There are IR divergences in the real correction, which are generated by phase space integration, and they should be finally canceled by the IR divergences appearing in the virtual correction. It is easy to realize[15] that, the terms $M_{\text{Real},i}^* M_{\text{Real},j}$ are IR finite for the phase space integral unless $M_{\text{Real},i}$ and $M_{\text{Real},j}$ are the amplitudes corresponding to Feynman diagrams in which a real gluon is emitted from an external on-shell line, e.g., here the first 8 diagrams in Fig.6. At this step, let us divide the cross section of the real correction into two parts as

$$d\sigma_{\text{Real}} = d\sigma_{\text{Real}}^{\text{IR}} + d\sigma_{\text{Real}}^{\text{IR-finite}}, \tag{7}$$

where $d\sigma_{\text{Real}}^{\text{IR}}$ contains the terms in $\sum_{i,j} M_{\text{Real},i}^* M_{\text{Real},j}$ only when $M_{\text{Real},i}$ and $M_{\text{Real},j}$ are the amplitudes corresponding to Feynman diagrams in which a real gluon is emitted from an external on-shell line. Namely we can formulate $d\sigma_{\text{Real}}^{\text{IR}}$ as

$$d\sigma_{\text{Real}}^{\text{IR}} = \frac{1}{4} \frac{1}{2s} \sum |M_{\text{Real}}^{\text{IR}}|^2 d\Phi_4 \tag{8}$$

where $M_{\text{Real}}^{\text{IR}}$ is the sum of the amplitudes corresponding to Feynman diagrams in which a real gluon is emitted from an external on-shell line. $d\sigma_{\text{Real}}^{\text{IR-finite}}$ contains the remaining terms in $\sum_{i,j} M_{\text{Real},i}^* M_{\text{Real},j}$, i.e., $(|M_{\text{Real}}|^2 - |M_{\text{Real}}^{\text{IR}}|^2)$. Due to the fact that there is no divergence in $\sigma_{\text{Real}}^{\text{IR-finite}}$, we can calculate it in 4-dimensional space-time directly.

In order to extract the IR divergences in $\sigma_{\text{Real}}^{\text{IR}}$ precisely so as to cancel the IR divergences in virtual correction precisely, we adopt the two-cutoff phase space slicing method[16]. By this method, the integration on the phase space is divided into two sectors through introducing a very soft cut $\delta_s (\ll 1)$ on the energy of the emitting gluon (p_4^0). Then,

$$d\sigma_{\text{Real}}^{\text{IR}} = d\sigma_{\text{Real}}^{\text{IR,soft}} + d\sigma_{\text{Real}}^{\text{IR,hard}}, \tag{9}$$

with the gluon g so soft being emitted by b or \bar{c} .

² We find that combinations Vertex-5 + Box-2, Vertex-6 + Box-3 + Pentagon-2 and Box-6 + Box-7 are IR finite. This is similar to the B_c production through Z-decay in Refs.[9, 10].

³ In literature, sometimes 'the NLO real correction' contains only the contributions from the process $e^+e^- \rightarrow B_c(B_c^*) + b + \bar{c} + g$

where

$$d\sigma_{\text{Real}}^{\text{IR,hard}} = \frac{1}{4} \frac{1}{2s} \sum |M_{\text{Real}}^{\text{IR}}|^2 d\Phi_4|_{p_4^0 > \delta_s \sqrt{s}/2}, \quad (10)$$

and

$$d\sigma_{\text{Real}}^{\text{IR,soft}} = \frac{1}{4} \frac{1}{2s} \sum |M_{\text{Real}}^{\text{IR}}|^2 d\Phi_4|_{p_4^0 < \delta_s \sqrt{s}/2}. \quad (11)$$

To calculate $\sigma_{\text{Real}}^{\text{IR,soft}}$, the eikonal approximation is adopted to deal with the amplitudes involved in $M_{\text{Real}}^{\text{IR}}$, where the terms of $\mathcal{O}(\delta_s)$ in $\sigma_{\text{Real}}^{\text{IR,soft}}$ have been neglected

[16, 17]. Under this approximation, the amplitude corresponding to the Feynman diagram where a real gluon emitted from an external line can be factorized as a Born factor multiplying an eikonal factor, and it is easy to check that the eikonal factors relating to the diagrams Real-5 and Real-6 of Fig.6 are canceled by the eikonal factors relating to the diagrams Real-7 and Real-8 of Fig.6 respectively at the leading order approximation in relative velocity $\mathcal{O}(v^0)$. Thus at last under the eikonal approximation we obtain

$$\sum |M_{\text{Real}}^{\text{IR}}|^2 = 4\pi\alpha_s C_F \mu^{2\epsilon} \left[\frac{-(p_2)^2}{(p_2 \cdot p_4)^2} + \frac{2p_2 \cdot p_3}{(p_2 \cdot p_4)(p_3 \cdot p_4)} - \frac{(p_3)^2}{(p_3 \cdot p_4)^2} \right] \sum |M_{\text{Born}}|^2. \quad (12)$$

Up-to corrections of $\mathcal{O}(\delta_s)$, the phase space for the soft sector can be factorized as [16]

$$d\Phi_4|_{p_4^0 < \delta_s \sqrt{s}/2} = d\Phi_3 \frac{d^{d-1}p_4}{2p_4^0 (2\pi)^{d-1}}|_{p_4^0 < \delta_s \sqrt{s}/2} \quad (13)$$

where $d\Phi_3$ denotes the element of the three-body phase space without emitting a gluon. Performing the integration over the momentum of emitting gluon (p_4) in the soft sector, the differential cross section

$$d\sigma_{\text{Real}}^{\text{IR,soft}} = d\sigma_{\text{Born}} \frac{\alpha_s}{\pi} \Gamma(1 + \epsilon) \left(\frac{4\pi\mu^2}{s} \right)^\epsilon \left(\frac{A}{\epsilon} + B \right) \quad (14)$$

is obtain[18], where

$$\begin{aligned} A &= C_F \left[1 - \frac{\kappa (p_2 \cdot p_3)}{\kappa^2 m_b^2 - m_c^2} \ln \left(\frac{\kappa^2 m_b^2}{m_c^2} \right) \right], \\ B &= C_F \left\{ - \left[1 - \frac{\kappa (p_2 \cdot p_3)}{\kappa^2 m_b^2 - m_c^2} \ln \left(\frac{\kappa^2 m_b^2}{m_c^2} \right) \right] \ln(\delta_s^2) + \frac{1}{2\beta_b} \ln \left(\frac{1 + \beta_b}{1 - \beta_b} \right) + \frac{1}{2\beta_{\bar{c}}} \ln \left(\frac{1 + \beta_{\bar{c}}}{1 - \beta_{\bar{c}}} \right) \right. \\ &\quad \left. + \frac{2\kappa (p_2 \cdot p_3)}{\kappa^2 m_b^2 - m_c^2} \left[\frac{1}{4} \ln^2 \left(\frac{u^0 - |\mathbf{u}|}{u^0 + |\mathbf{u}|} \right) + \text{Li}_2 \left(1 - \frac{u^0 + |\mathbf{u}|}{v} \right) + \text{Li}_2 \left(1 - \frac{u^0 - |\mathbf{u}|}{v} \right) \right]_{u=p_3}^{u=\kappa p_2} \right\}, \quad (15) \end{aligned}$$

here

$$\begin{aligned} \beta_b &= \sqrt{1 - m_b^2/(p_2^0)^2}, \\ \beta_{\bar{c}} &= \sqrt{1 - m_c^2/(p_3^0)^2}, \quad (16) \end{aligned}$$

$$v = \frac{\kappa^2 m_b^2 - m_c^2}{2(\kappa p_2^0 - p_3^0)}, \quad (17)$$

and

$$\kappa = \frac{p_2 \cdot p_3 + \sqrt{(p_2 \cdot p_3)^2 - m_b^2 m_c^2}}{m_b^2}. \quad (18)$$

It can be checked precisely that the $1/\epsilon$ -terms in $d\sigma_{\text{Real}}^{\text{IR,soft}}$ defined by Eq.(14) are just canceled by those infrared $1/\epsilon$ -terms remained by the virtual correction Eq.(3).

Since there is no IR divergence in $d\sigma_{\text{Real}}^{\text{IR,hard}}$ due to the constraint $p_4^0 > \delta_s \sqrt{s}/2$, so we can calculate it in 4-dimensional space-time safely. Summing up $\sigma_{\text{Real}}^{\text{IR-finite}}$, $\sigma_{\text{Real}}^{\text{IR,soft}}$ and $\sigma_{\text{Real}}^{\text{IR,hard}}$, the requested σ_{Real} is obtained. Then with the Eqs.(2,3,7), the cross section σ_{NLO} , the NLO QCD production, of the process $e^+ + e^- \rightarrow B_c(B_c^*) + b + \bar{c} + X$ may be computed directly.

$\cos\theta$	-0.8	-0.6	-0.4	-0.2	0	0.2	0.4	0.6	0.8
$d\sigma/d\cos\theta(B_c, LO)$	1.066	0.892	0.759	0.667	0.617	0.608	0.639	0.711	0.825
$d\sigma/d\cos\theta(B_c, NLO)$	1.606	1.346	1.150	1.014	0.939	0.924	0.969	1.075	1.242
$K(B_c)$	1.506	1.509	1.515	1.520	1.522	1.520	1.516	1.512	1.505
$d\sigma/d\cos\theta(B_c^*, LO)$	1.507	1.254	1.060	0.926	0.853	0.839	0.884	0.990	1.156
$d\sigma/d\cos\theta(B_c^*, NLO)$	1.990	1.662	1.414	1.240	1.144	1.125	1.183	1.317	1.529
$K(B_c^*)$	1.320	1.325	1.334	1.339	1.341	1.341	1.338	1.330	1.323

TABLE III: The LO and NLO differential cross sections $\frac{d\sigma}{d\cos\theta}$ (in pb) of $e^-e^+ \rightarrow B_c(B_c^*) + b + \bar{c} + X$ and their ratio at various scattering angles θ at the Z pole ($\mu = 2m_b$).

IV. NUMERICAL RESULTS

For numerical calculations, the necessary input parameters are taken:

$$\begin{aligned}
m_b &= 4.9 \text{ GeV}, m_c = 1.5 \text{ GeV}, m_Z = 91.1876 \text{ GeV}, \\
\sin^2\theta_w &= 0.231, \alpha = 1/128, \Gamma_Z = 2.4952 \text{ GeV} \\
|R_S(0)|^2 &= 1.642 \text{ GeV}^3,
\end{aligned} \tag{19}$$

$\alpha = \alpha(m_Z)$ is the electromagnetic coupling constant at $\mu = m_Z$; $R_S(0)$ is the radial wave function at the origin for $B_c(B_c^*)$, which can be taken from the potential model[2]. We apply the two-loop formula for the strong coupling constant $\alpha_s(\mu)$:

$$\alpha_s(\mu) = \frac{4\pi}{\beta_0 \ln(\mu^2/\Lambda_{QCD}^2)} \left[1 - \frac{\beta_1 \ln \ln(\mu^2/\Lambda_{QCD}^2)}{\beta_0^2 \ln(\mu^2/\Lambda_{QCD}^2)} \right], \tag{20}$$

where $\beta_1 = \frac{34}{3}C_A^2 - 4C_F T_F n_f - \frac{20}{3}C_A T_F n_f$ is the two-loop coefficient of the QCD β -function. According to

Note that in the calculations here, we use FeynArts[20] for generating Feynman diagrams and amplitudes, FeynCalc[21] and FeynCalcFormLink[22] for carrying out the trace of color and Dirac matrices; while Apart[23] and FIRE[24] for conducting partial fraction and integration-by-parts (IBP) reduction. All the one-loop integrals are reduced into master integrals and the master integrals are computed in terms of LoopTools[25] numerically. The final phase-space integrations are computed with the help of the soft-ware Vegas[26].

The numerical results of the total cross sections at the colliding center-mass energy m_Z as well as the so-called K -factor for the productions $e^+e^- \rightarrow B_c + b + \bar{c} + X$ and $e^+e^- \rightarrow B_c^* + b + \bar{c} + X$ with two different renormalization scales, $\mu = 2m_b$ and $\mu = m_Z/2$, are put into the tables: TABLE I and TABLE II respectively, and the precise dependence of the cross sections on the renormalization scale μ for LO and NLO QCD is presented in Fig.7. It is shown in Fig.7 that the cross section of the production $e^+e^- \rightarrow B_c(B_c^*) + b + \bar{c} + X$ at Z pole

$\alpha_s(m_Z) = 0.1185$ [19], we obtain $\Lambda_{QCD}^{n_f=5} = 0.233 \text{ GeV}$.

μ	$\alpha_s(\mu)$	$\sigma_{LO}(\text{pb})$	$\sigma_{NLO}(\text{pb})$	$K \equiv \sigma_{NLO}/\sigma_{LO}$
$2m_b$	0.180	1.576	2.387	1.515
$m_Z/2$	0.132	0.847	1.587	1.874

TABLE I: The cross section of $e^+e^- \rightarrow B_c + b + \bar{c} + X$ at Z-pole under two typical renormalization scales.

μ	$\alpha_s(\mu)$	$\sigma_{LO}(\text{pb})$	$\sigma_{NLO}(\text{pb})$	$K \equiv \sigma_{NLO}/\sigma_{LO}$
$2m_b$	0.180	2.204	2.930	1.329
$m_Z/2$	0.132	1.185	2.059	1.738

TABLE II: The cross section of $e^+e^- \rightarrow B_c^* + b + \bar{c} + X$ at Z-pole under two typical renormalization scales.

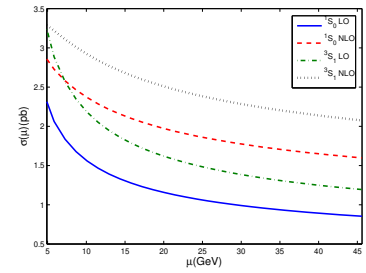


FIG. 7: The dependence of the LO and NLO cross sections at the Z pole on the renormalization scale μ .

decreases by 46%(46%) at LO degree but by 34% (30%) at NLO degree when the renormalization scale μ changes from $2m_b$ to $m_Z/2$. Namely the renormalization scale dependence is weakened a lot from LO to NLO correction. Whereas the dependence on the renormalization scale μ is still quite large for NLO, thus it is considered that

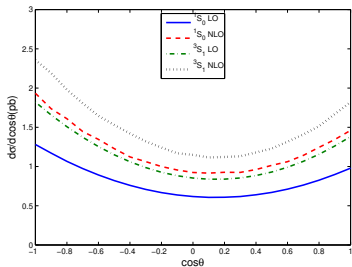


FIG. 8: The LO and NLO differential cross sections $\frac{d\sigma}{d\cos\theta}$ with $\mu = 2m_b$ for the processes $e^-e^+ \rightarrow B_c(B_c^*) + b + \bar{c} + X$ at the Z pole.

to suppress the dependence on μ further, higher order corrections in QCD for the considered production are requested.

Moreover, we also calculate the differential cross sections $d\sigma/d\cos\theta$, $d\sigma/dz$ and the relevant K -factor as well. θ is the angle between the momenta of the electron in initial state and the meson $B_c(B_c^*)$ in final state at the center-of-mass system and z is the 'energy-fraction' defined as $2k \cdot p_1/s$ (k is the momentum carried by Z boson).

The differential cross sections $d\sigma/d\cos\theta$ for the production of $B_c(B_c^*)$ meson at LO and NLO, and the K factor as well are put in TABLE III. The differential cross sections $d\sigma/d\cos\theta$ with renormalization scale $\mu = 2m_b$ are presented in Fig.8. One can see from Fig.8 that the distribution $\frac{d\sigma}{d\cos\theta}$ changes some (almost a common factor K as shown in TABLE III) due to the NLO QCD corrections.

The energy-fraction distribution $\frac{d\sigma}{dz}$ for the $B_c(B_c^*)$ meson production is also computed and put in Fig.9. The NLO QCD correction shifts the maximum point of energy-fraction distribution to smaller energy some.

To see the asymmetry of the production caused by electroweak interaction, the differential cross sections $d\sigma/d\cos\theta$ for the production varying with the values of the electroweak mixing angle $\sin^2\theta_w$ are computed and presented in Fig.10. As pointed out above, the NLO QCD corrections almost do not change the shape of the differential angle distributions for the $B_c(B_c^*)$ production except the K factor, so here the differential cross sections for NLO with $\mu = 2m_b$ is represented by the relevant LO differential cross sections multiplying a K -factor 1.515 approximately. From Fig.10 one can see that the shape of the angle distribution is sensitive to the value of $\sin^2\theta_w$. It means that one can measure the value of $\sin^2\theta_w$ through observing the angle distribution of the B_c meson.

To see the variation of the total cross sections with the collision energy around m_Z by 5 GeV at LO and NLO

level, we also compute them with $\mu = 2m_b$ and put the results in TABLE.IV.

We should here point out that, on one hand, from the total cross section of the process $e^+e^- \rightarrow B_c(B_c^*) + b +$

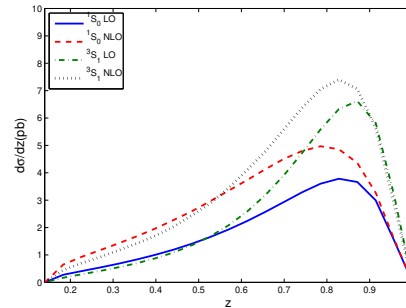


FIG. 9: The LO and NLO differential cross sections $\frac{d\sigma}{dz}$ for the process $e^-e^+ \rightarrow B_c(B_c^*) + b + \bar{c} + X$ at the Z pole. The renormalization scale has been set as $\mu = 2m_b$.

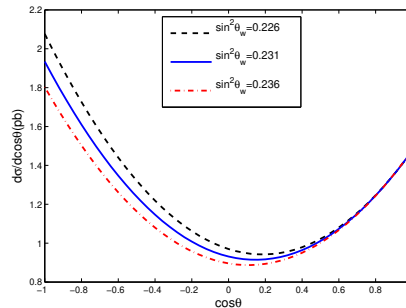


FIG. 10: The differential cross sections $\frac{d\sigma}{d\cos\theta}$ for the B_c production at the Z pole under various values of $\sin^2\theta_w$.

$\bar{c} + X$ at Z pole, the relevant partial decay widths for the decay $Z \rightarrow B_c(B_c^*) + b + \bar{c} + X$ can be easily 'read out' and, on the other hand, in the literature there are results on the partial decay widths for the decay $Z \rightarrow B_c(B_c^*) + b + \bar{c} + X$ at LO and NLO[9, 10], thus we need to compare our results with theirs. In Appendix-A, the way how to 'read out' the partial decay widths for the decay $Z \rightarrow B_c(B_c^*) + b + \bar{c} + X$ from the production $e^+ + e^- \rightarrow B_c(B_c^*) + b + \bar{c} + X$ at Z pole is derived and in Appendix-B careful comparisons with those of Refs.[9, 10] are made. The situation on the comparisons is that when we take the same input parameters as those adopted in Refs.[9, 10], our NLO partial decay width for $Z \rightarrow B_c + b + \bar{c} + X$ is bigger than that in Ref.[9], but the NLO partial decay width for the decay $Z \rightarrow B_c^* + b + \bar{c} + X$ (and all of the LO partial decay widths are consistent with those in Ref.[10].

Since in the above calculations the contributions from annihilation of electron and positron into virtual γ are ig-

nored, which correspond to those Feynman diagrams by

$(\sqrt{s} - m_Z)(\text{GeV})$	-5	-2.5	-1.5	-0.8	-0.4	-0.2	0	0.2	0.4	0.8	1.5	2.5	5
B_c (LO)	0.09	0.30	0.63	1.10	1.42	1.53	1.58	1.54	1.44	1.13	0.66	0.32	0.10
B_c (NLO)	0.13	0.46	0.95	1.66	2.13	2.32	2.39	2.33	2.18	1.71	1.00	0.49	0.15
B_c^* (LO)	0.12	0.42	0.88	1.54	1.98	2.14	2.20	2.16	2.02	1.59	0.92	0.46	0.14
B_c^* (NLO)	0.16	0.56	1.17	2.04	2.64	2.84	2.93	2.87	2.67	2.11	1.23	0.60	0.18

TABLE IV: The cross section (in pb) of $e^-e^+ \rightarrow B_c(B_c^*) + b + \bar{c} + X$ at various collision energies around m_Z ($\mu = 2m_b$).

$(\sqrt{s} - m_Z)(\text{GeV})$	-5	-2.5	-1.5	-0.8	-0.4	-0.2	0	0.2	0.4	0.8	1.5	2.5	5
B_c	0.18	-0.35	-0.63	-0.53	0.06	0.33	0.79	1.24	1.64	2.11	2.21	1.91	1.39
B_c^*	0.19	-0.53	-0.92	-0.78	-0.12	0.41	1.04	1.67	2.22	2.88	3.01	2.60	1.88

TABLE V: The contributions (in fb) from photon propagation diagrams at different collision energies around m_Z .

replacing the Z -boson with a photon in Fig.1. In order to see the contributions, especially, the interference of the Z -boson and photon annihilations, we compute the contributions from two parts: the square of the amplitude via annihilation to γ and the $\gamma - Z$ interference, and put the results in TABLE V. One may from the results TABLE V see that the contributions from the γ annihilation and the $\gamma - Z$ interference around the resonance Z -pole is very small in comparison with the contributions from the Z -boson annihilation.

V. DISCUSSIONS AND CONCLUSION

We have calculated the NLO QCD corrections to the production of $B_c(B_c^*)$ meson at an e^+e^- collider running near the Z pole. The results show that the NLO corrections are significant. The dependence on the renormalization scale μ for the cross sections at NLO level is depressed in comparison with LO results. Precisely, the total cross section for the $B_c(B_c^*)$ production at Z -pole decreases about 46%(46%) for LO, and about 34%(30%) for NLO when μ changes from $2m_b$ to $m_Z/2$. Namely, the dependence of the cross sections on the renormalization scale μ for NLO correction is still not small, so the higher order corrections are requested.

In addition to the total cross section, the differential cross sections on angle and energy fraction distributions of the produced $B_c(B_c^*)$ meson are computed and analyzed too. It is found that the K -factor for NLO QCD corrections to LO QCD calculations changes slightly with the angle, but the energy distribution changes sizable: the maximum is shifted to smaller energy fraction (see TABLE. III, Figs. 8 and 9). The characters of the production in the differential cross sections on angle up-to NLO may be potentially used to measure the electroweak mixing angle $\sin^2\theta_w$.

According to the present NLO calculations, as the conclusion obtained by LO calculations, to study the production $e^+e^- \rightarrow B_c(B_c^*) + b + \bar{c} + X$ experimentally, even at Z -pole, a luminosity higher than $10^{35} \text{ cm}^{-2}\text{s}^{-1}$ for the

collider is needed, because of the cross sections being in the order $\mathcal{O}(pb)$ and the comparatively small efficiency in detecting the meson $B_c(B_c^*)$.

Acknowledgments: We thank Jian-Xiong Wang and Rong Li for helpful discussions. This work was supported in part by Nature Science Foundation of China (NSFC) under Grant No. 11275243, No. 11275036, No. 11447601, No. 11535002 and No. 11675239

Appendix

A. The relation between production $\sigma(e^+e^- \rightarrow B_c(B_c^*) + b + \bar{c} + X)$ at Z -pole and the decay $\Gamma(Z^0 \rightarrow B_c(B_c^*) + b + \bar{c} + X)$

The total cross section of the process $e^+e^- \rightarrow Z^0 \rightarrow B_c(B_c^*) + b + \bar{c} + X$ can be represented as

$$\sigma = \frac{1}{4} \frac{1}{2s} \frac{L^{\mu\nu} H_{\mu\nu}}{(s - m_Z^2)^2 + m_Z^2 \Gamma_Z^2}, \quad (21)$$

where Γ_Z is the total width of the boson Z , $L^{\mu\nu}$ is the leptonic tensor and

$$L^{\mu\nu} = a [q_1^\mu q_2^\nu + q_2^\mu q_1^\nu - (s/2)g^{\mu\nu}] + ib\epsilon^{\mu\nu\lambda\tau} q_{1\lambda} q_{2\tau}, \quad (22)$$

here

$$a = \frac{e^2(1 - 4\sin^2\theta_w + 8\sin^4\theta_w)}{2\sin^2\theta_w \cos^2\theta_w},$$

$$b = \frac{e^2(1 - 4\sin^2\theta_w)}{2\sin^2\theta_w \cos^2\theta_w}. \quad (23)$$

$H_{\mu\nu}$ is the hadronic tensor, which has been performed the phase space integral. $H_{\mu\nu}$ can only depend on k , and has following form

$$H_{\mu\nu} = H_1(s)g_{\mu\nu} + H_2(s)k_\mu k_\nu / s, \quad (24)$$

where $H_1(s)$ and $H_2(s)$ are scalar functions. Because there's no UV or IR divergence after considering the renormalization and the real correction, $H_1(s)$ and $H_2(s)$

are free of UV and IR divergences. Thus, all the derivations in the appendix are performed in 4 dimensions. According to Eqs.(21), (22) and (24), we can obtain the cross section at Z pole

$$\sigma = -\frac{aH_1(m_Z^2)}{8m_Z^2\Gamma_Z^2}, \quad (25)$$

here we have used $s = m_Z^2$.

The decay width of the process $Z^0 \rightarrow B_c(B_c^*) + b + \bar{c} + X$ is

$$\Gamma = \frac{1}{3} \frac{1}{2m_Z} \Pi^{\mu\nu} H_{\mu\nu}, \quad (26)$$

where

$$\Pi^{\mu\nu} = -g^{\mu\nu} + k^\mu k^\nu / m_Z^2, \quad (27)$$

then we obtain

$$\Gamma = -\frac{H_1(m_Z^2)}{2m_Z}. \quad (28)$$

According to Eqs.(25) and (28), we obtain the relation

$$\Gamma = \frac{4m_Z\Gamma_Z^2}{a}\sigma. \quad (29)$$

From Eq.(29), one can obtain the decay width of the process $Z^0 \rightarrow B_c(B_c^*) + b + \bar{c} + X$ through the total cross

section of the process $e^+e^- \rightarrow B_c(B_c^*) + b + \bar{c} + X$ which calculated in the present paper, and vice versa. But from the decay partial width $\Gamma(Z^0 \rightarrow B_c(B_c^*) + b + \bar{c} + X)$, the differential cross section $d\sigma(e^+e^- \rightarrow B_c(B_c^*) + b + \bar{c} + X)$ for the production cannot be obtained.

B. To compare the results for the decay $Z^0 \rightarrow B_c(B_c^*) + b + \bar{c} + X$ up-to NLO

There are NLO correction calculations on the decay $Z^0 \rightarrow B_c(B_c^*) + b + \bar{c} + X$ in Refs.[9, 10], so let us do the comparisons between theirs and those reduced from our calculation on the production $e^+e^- \rightarrow B_c(B_c^*) + b + \bar{c} + X$ in terms of Appendix-A.

The two-cutoff phase space slicing method for the phase space integration by introducing δ_s [13] is used as indicated by Eqs.(9,10,11) and δ_s is fixed as 10^{-6} finally according to the requirement for the method. Hence for precise comparisons it would be better that the errors generated by our calculations should be presented. Moreover, in order to compare the results in Refs.[9, 10] with ours, we take the same parameters as those taken in Refs.[9, 10], compute the decay widths keeping the errors and put the results in TABLES VI VII.

μ	$\Gamma^{\text{LO+Vir+IR,soft}}$	$\Gamma_{\text{Real}}^{\text{IR,hard}}$	$\Gamma_{\text{Real}}^{\text{IR-finite}}$	Γ_{NLO}	$\Gamma_{\text{NLO}}(\text{Ref.}[9])$
$2m_b$	-567.60 ± 0.05	492.21 ± 0.07	186.44 ± 0.02	111.05 ± 0.09	78.45
$m_Z/2$	-199.61 ± 0.02	200.05 ± 0.03	75.78 ± 0.01	76.22 ± 0.04	62.53

TABLE VI: The decay widths (in keV) of $Z \rightarrow B_c + b + \bar{c} + X$ with the same values of input parameters as Ref.[9], where the numbers in the last column are copied from Ref.[9]. For the NLO widths, the statistical errors from numerical phase space integrals are also given.

μ	$\Gamma^{\text{LO+Vir+IR,soft}}$	$\Gamma_{\text{Real}}^{\text{IR,hard}}$	$\Gamma_{\text{Real}}^{\text{IR-finite}}$	Γ_{NLO}	$\Gamma_{\text{NLO}}(\text{Ref.}[10])$
$2m_b$	-632.78 ± 0.03	550.53 ± 0.07	200.73 ± 0.03	118.48 ± 0.09	118.77
$m_Z/2$	-218.34 ± 0.02	221.90 ± 0.03	80.91 ± 0.02	84.47 ± 0.05	84.60

TABLE VII: The decay widths (in keV) of $Z \rightarrow B_c^* + b + \bar{c} + X$ with the same values of input parameters as Ref.[10], where the numbers in the last column are copied from Ref.[10]. For the NLO widths, the statistical errors from numerical phase space integrals are also given.

From the tables, one may see that the results for NLO correction of B_c production in [9] are different from ours,

but those for NLO correction of B_c^* production in [10] are consistent with ours.

[1] F. Abe, et al. (CDF Collaboration), Observation of the B_c Meson in $p\bar{p}$ Collisions at $\sqrt{s} = 1.8\text{TeV}$, Phys. Rev.

Lett. **81**, 2432 (1998); Observation of B_c mesons in $p\bar{p}$

- collisions at $\sqrt{s} = 1.8\text{TeV}$, Phys. Rev. D **58**, 112004 (1998).
- [2] E.J. Eichten and C. Quigg, Mesons with beauty and charm: Spectroscopy, Phys.Rev. D**49**, 5845 (1994).
- [3] G.T. Bodwin, E. Braaten and G.P. Lepage, Rigorous QCD analysis of inclusive annihilation and production of heavy quarkonium, Phys. Rev. D **51**, 1125 (1995) [Erratum-ibid. D **55**, 5853 (1997)].
- [4] N. Brambilla, et al. Heavy Quarkonium Physics, CERN-2005-005 20 June 2005, arXiv: hep-ph/0412158.
- [5] N. Brambilla, et al. Heavy quarkonium: progress, puzzles, and opportunities, Eur. Phys. J. C **71**, 1534 (2011) and references therein.
- [6] C.-H Chang and Y.-Q Chen, The Production of B_c or \bar{B}_c associated with two heavy quark jets in Z^0 boson decay, Phys. Rev. D **46**, 3845 (1992); Erratum, Phys. Rev. D **50**, 6013 (1994); The B_c and \bar{B}_c mesons accessible to experiments by Z^0 boson decay, Phys. Letts. B **284**, 127-132 (1992).
- [7] P. Abreu, et al (DELPHI Collaboration), Search for the B_c meson, Phys. Letts. B **398**, 207 (1997); R. Barate, et al (ALEPH Collaboration), Search for the B_c meson in hadronic Z^0 decay, Phys. Letts. B **402**, 213 (1997); K. Ackerstaff, et al (OPAL Collaboration), Search for the B_c meson in hadronic Z^0 decay, Phys. Letts. B **420**, 157 (1998).
- [8] X.-C. Zheng, C.-H. Chang and Z. Pan, Production of doubly heavy-flavored hadrons at e^+e^- colliders, Phys. Rev. D **93**, 034019 (2016).
- [9] C.-F. Qiao, L.-P. Sun, R.-L. Zhu, The NLO QCD Corrections to B_c Meson Production in Z^0 Decays, JHEP **08**, 131 (2011).
- [10] J. Jiang, L.-B. Chen, C.-F. Qiao, QCD NLO corrections to inclusive B_c^* production in Z^0 decays, Phys. Rev. D**91**, 034033 (2015).
- [11] M. Beneke and V.A. Smirnov, Asymptotic expansion of Feynman integrals near threshold, Nucl. Phys. B**522**, 321 (1998).
- [12] J.G. Korner, D. Kreimer and K. Schilcher, A Practicable γ_5 -scheme in dimensional regularization, Z. Phys. C**54**, 503 (1992).
- [13] T. Kinoshita, Mass Singularities of Feynman Amplitudes, J. Math. Phys. **3**, 650 (1962).
- [14] S. Dittmaier, Separation of soft and collinear singularities from one-loop N-point integrals, Nucl. Phys. B**675**, 447 (2003).
- [15] G. Grammer, Jr. and D. R. Yennie, Improved Treatment for the Infrared-Divergence Problem in Quantum Electrodynamics, Phys. Rev. D **8**, 4332 (1973).
- [16] B.W. Harris and J.F. Owens, Two cutoff phase space slicing method, Phys. Rev. D **65**, 094032 (2002).
- [17] A. Bassetto, M. Ciafaloni, and G. Marchesini, Jet Structure and Infrared Sensitive Quantities in Perturbative QCD, Phys. Rept. **100**, 201 (1983).
- [18] A. Denner, Techniques for the Calculation of Electroweak Radiative Corrections at the One-loop Level and Results for W-physics at LEP-200, Fortschr. Phys. **41**, 307 (1993).
- [19] K.A. Olive, et al. (Particle Data Group), Review of particle physics, Chin. Phys. C**38**, 090001 (2014).
- [20] T. Hahn, Generating Feynman diagrams and amplitudes with FeynArts 3, Comput. Phys. Commun **140**, 418 (2001).
- [21] R. Mertig, M. Bohm and A. Denner, Feyn Calc - Computer-algebraic calculation of Feynman amplitudes, Comput. Phys. Commun **64**, 345 (1991).
- [22] F. Feng and R. Mertig, FormLink/FeynCalcFormLink: Embedding FORM in Mathematica and FeynCalc, arXiv:1212.3522.
- [23] F. Feng, \$Apart: A Generalized Mathematica Apart Function, Comput. Phys. Commun **183**, 2158 (2012).
- [24] A.V. Smirnov, Algorithm FIRE - Feynman Integral Reduction, J. High Energy Phys. **10**, 107 (2008).
- [25] T. Hahn and M. Perez-Victoria, Automatized one loop calculations in four-dimensions and D-dimensions, Comput. Phys. Commun **118**, 153 (1999).
- [26] G.P. Lepage, A New Algorithm for Adaptive Multidimensional Integration, J. Comp. Phys. **27**, 192 (1978).